



Predicting the Sound Transmission Loss of Sandwich Panels by Statistical Energy Analysis Approach

Tongan Wang^{1,*}, Shan Li¹, Shankar Rajaram¹, Steven R. Nutt¹

1. University of Southern California, 3651 Watt Way, VHE 602, Los Angeles, CA 90089

Abstract: A statistical energy analysis (SEA) approach is used to predict the sound transmission loss (STL) of sandwich panels numerically. Unlike conventional SEA studies of the STL of sandwich panels, which consider only the antisymmetric (bending) motion of the sandwich panel, the present approach accounts for both antisymmetric and symmetric (dilatational) motions. Using the consistent higher-order sandwich plate theory, the wave numbers of the waves propagating in the sandwich panel were calculated. Using these wave numbers, the wave speed of the propagating waves, the modal density, and the radiation efficiency of the sandwich panels were determined. Finally, the sound transmission losses of two sandwich panels were calculated and compared with the experimentally measured values, as well as with conventional SEA predictions. The comparisons with the experimental data showed good agreement, and the superiority of the present approach relative to other approaches is discussed and analyzed.

Key words: sound transmission loss, sandwich panel, statistical energy analysis, higher-order theory

*Corresponding author: tonganw@yahoo.com

1. Introduction

Sandwich constructions are widely used in engineering applications because of the extremely high stiffness-to-mass ratio. The same high stiffness-to-mass ratio that imparts mechanical efficiency also imparts efficient transmission and radiation of acoustic noise, posing a serious problem for some

Please cite this article as: Wang T, Li S, Rajaram S, Nutt SR. **Predicting the Sound Transmission Loss of Sandwich Panels by Statistical Energy Analysis Approach**. *ASME. J. Vib. Acoust.* 2010;132(1):011004-011004-7. doi:10.1115/1.4000459.



applications. To address this problem, engineers have attempted to identify optimal designs for sandwich panels that balance mechanical and acoustical properties. In one such study, Dym and Lang [1] concluded that asymmetric sandwich panel designs could enhance the sound transmission loss of sandwich panels, albeit at the cost of higher mass density. Thus, the present study focuses on symmetric sandwich panels, in which the two face sheets are identical.

Vibro-acoustic studies of symmetric sandwich panels have been carried out both theoretically [1-10] and numerically [11-12]. A detailed review of theoretical approaches was given in Ref. 10. Comparing with the theoretical methods, numerical approaches have more practical importance, i.e., when the sandwich panel is part of a large structure and the interactions between structures are important. Conventional numerical methods include the finite element method (FEM) and boundary element method (BEM). However, the utility of FEM at high frequency is generally limited because of the vast number of vibration modes [11]. For the same reason, efforts to simulate vibration modes using BEM have encountered similar limitations at high frequencies [12].

In contrast to the above-mentioned methods, statistical energy analysis (SEA) is well-suited to the analysis of high-frequency structural response under acoustic excitation, particularly for large structures [13]. SEA is based on the statistics of vibration modes. The modal densities of sandwich panels have been studied by Renji et al. [14]. The prediction of STL of homogeneous panels using SEA is well-documented [15-16]. By treating the sandwich panel as a single homogeneous layer, this approach has been used to predict the STL of sandwich panels [17]. However, for sandwich panel vibrations, the two face sheets do not necessarily move in phase with each other. In fact, this distinctive feature can cause dilatational motion of the two face sheets [5]. The shortcomings of this SEA approach stem from the fact that only the antisymmetric (bending) motion of the structure was

Please cite this article as: Wang T, Li S, Rajaram S, Nutt SR. **Predicting the Sound Transmission Loss of Sandwich Panels by Statistical Energy Analysis Approach.** *ASME. J. Vib. Acoust.* 2010;132(1):011004-011004-7. doi:10.1115/1.4000459.



considered, while neglecting this symmetric (dilatational) motion. The antisymmetric and symmetric motions of the sandwich panel will be considered in more detail in Sec. 2.

Ghinet et al. [18] used SEA method to calculate the transmission loss of curved sandwich panels by treating them as general composite laminates. The dispersion behavior of the panel was calculated from the dynamic equations, with which the modal density, radiation efficiency, and transmission loss of the composite panels were predicted. However, the displacement field of any discrete layer of the panel was of Mindlin's type, and was assumed to be incompressible in the normal direction, which neglected the dilatational motion of the sandwich panel. This study was further extended recently to predict the sound transmission from diffuse field into infinite sandwich composite and laminate composite cylinders [19].

One approach to solve for the limitation of the dilatational motion of sandwich panels involves the use of higher-order theory. A recent report described the use of consistent higher-order sandwich plate theory (HSAPT), which considers both the antisymmetric and symmetric motions [20]. HSAPT was both accurate and efficient when used to describe and predict dynamical motions of sandwich panels. In the present paper, this approach will be briefly reviewed, and then combined with SEA to predict the sound transmission loss of sandwich panels. The major difference between the present approach and previous SEA of sandwich panels is the incorporation of the dilatational modes in the study.

The modal density, and the coupling and dissipation loss factors form the basic parameters required for SEA. The accuracy of the prediction strongly depends on the accuracy with which these parameters are calculated. In the present paper, the wave numbers of the antisymmetric and symmetric motions of the sandwich panel are predicted using the HSAPT approach. Subsequently,

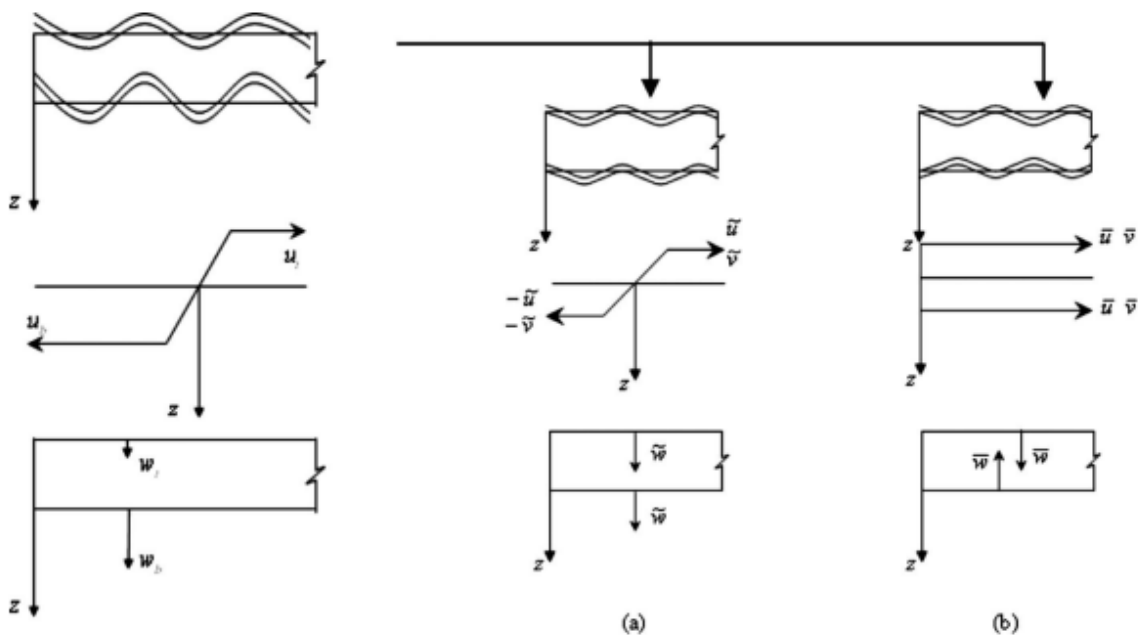
Please cite this article as: Wang T, Li S, Rajaram S, Nutt SR. **Predicting the Sound Transmission Loss of Sandwich Panels by Statistical Energy Analysis Approach.** ASME. *J. Vib. Acoust.* 2010;132(1):011004-011004-7. doi:10.1115/1.4000459.



the radiation efficiencies of the antisymmetric motion of the sandwich panel is calculated by Lyon and DeJong's formula [13] with modifications. Assumptions are made about the radiation efficiency of the symmetric modes. Finally, the sound transmission loss is predicted and compared with both experimental data and other numerical results.

2. Dynamic Equations

When a homogeneous single-layer panel is vibrating, the transverse velocity remains constant through the thickness of the panel. For a sandwich panel, however, the transverse velocities of the face sheets on each side of the core in most cases are not equal, as illustrated in the figure on the left of Fig. 1, where u_i, w_i ($i = t(\text{top}), b(\text{bottom})$) are the in-plane and transverse displacements of the centroid line of the face sheets, respectively. Therefore, the normal velocities of the face sheets have to be modeled separately.



Please cite this article as: Wang T, Li S, Rajaram S, Nutt SR. **Predicting the Sound Transmission Loss of Sandwich Panels by Statistical Energy Analysis Approach.** *ASME. J. Vib. Acoust.* 2010;132(1):011004-011004-7. doi:10.1115/1.4000459.



Figure 1: Transformation of the general motion of the sandwich panel to the antisymmetric and symmetric motions of the same panel: (a) antisymmetric (bending) and (b) symmetric (dilatational) motions

When a homogeneous single-layer panel is vibrating, the transverse velocity remains constant through the thickness of the panel. For a sandwich panel, however, the transverse velocities of the face sheets on each side of the core in most cases are not equal, as illustrated in the figure on the left of Fig. 1, where u_i, w_i ($i = t(\text{top}), b(\text{bottom})$) are the in-plane and transverse displacements of the centroid line of the face sheets, respectively. Therefore, the normal velocities of the face sheets have to be modeled separately.

In the HSAPT approach [20], the shear strains in the thin face sheets are neglected, and the in-plane stiffness of the core is also neglected. The height of the core may change under loading, and the core cross section does not remain planar. The interface layers between the face sheets and the core are assumed to provide perfect continuity of the deformations at the interfaces. Based on these assumptions, the displacement of the core can be expressed in terms of the displacements of the face sheets and the shear stress of the core, and most importantly, the core displacement varies *nonlinearly* in the thickness direction of the core.

The general motion of the sandwich panel can be transformed using Eqs. (1) and (2) into two types of motions with simpler physical meanings, namely, antisymmetric and symmetric motions, as shown in Figs. 2(a) and 2(b)

$$u_i = \bar{u} \pm \tilde{u} \tag{1}$$

$$w_i = \tilde{w} \pm \bar{w} \tag{2}$$



where \bar{u}, \bar{w} and \tilde{u}, \tilde{w} are the symmetric and antisymmetric displacement components of the face sheets, respectively, and the plus and minus signs are used for the upper and lower face sheets, respectively.

The antisymmetric motion can also be considered as the bending motion of the sandwich panel. Here, the two face sheets move in phase with each other, as in the pure bending motion of a single-layer panel. On the other hand, in the symmetric motion of the sandwich panel, which is also called dilatational motion, the two face sheets move out of phase with each other (see Fig. 2). In both cases, the amplitudes of the two face sheets are equal. When the two face sheets of the sandwich panel are identical, the antisymmetric and symmetric motions of the sandwich panel can be treated separately. The symmetric motion of the sandwich panel is governed by the displacement of the symmetric motion of the face sheets, expressed as

$$b(2\rho d + \rho_c c) \ddot{u}_s - 2Ebdu_{s,xx} - \frac{1}{6}b\rho_c c(c + 3d) \ddot{w}_{s,x} = 0 \quad (3)$$

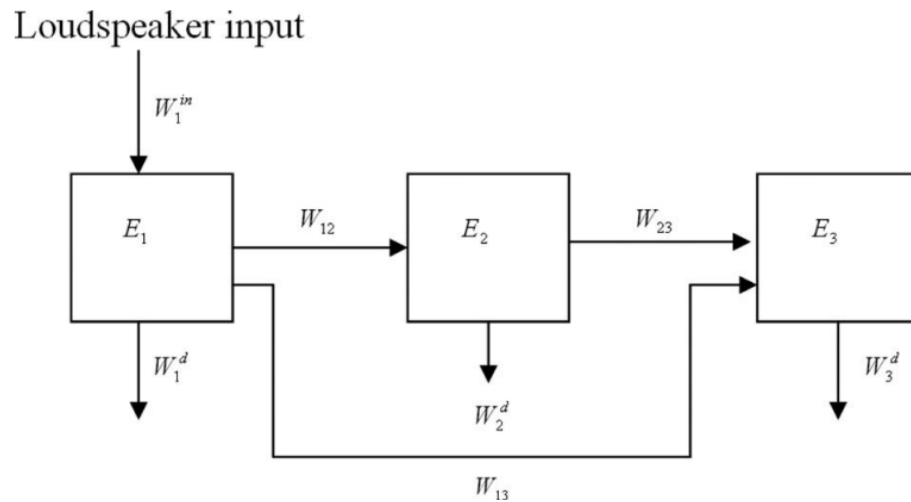


Figure 2: Block diagram illustrating the power flow in three-way coupled systems, where W_i^{in} in represents the input power to system 1, W_i^d is the power dissipated in system i , W_{ij} denotes the net power lost by system i through coupling to system j , and E_i is the total energy in system i



$$\begin{aligned}
 & -\frac{1}{6}b\rho_c c(c+3d)\ddot{u}_{s,x} + \frac{1}{60}(120\rho l + 15b\rho_c c d^2 + 10b\rho_c c^2 d \\
 & \quad + 2b\rho_c c^3)\ddot{w}_{s,xx} - \frac{1}{3}b(6\rho d + \rho_c c)\ddot{w}_s - (4E_c b/c)w_s - 2EIw_{s,xxxx} \\
 & = p_b - p_t
 \end{aligned} \tag{4}$$

Likewise, the antisymmetric motion are in terms of the displacements of the antisymmetric motion and the shear stress of the core, expressed as

$$\begin{aligned}
 & -\frac{1}{35}b(70\rho d + 17\rho_c c)\ddot{u}_a + 2Ebd u_{a,xx} + \frac{1}{70}b\rho_c c(3c + 17d)\ddot{w}_{a,x} \\
 & \quad - \frac{3}{70}(b\rho_c c^2/G_c)\ddot{\tau} + 2b\tau = 0
 \end{aligned} \tag{5}$$

$$\begin{aligned}
 & -\frac{1}{70}b\rho_c c(3c + 17d)\ddot{u}_{a,x} + \frac{1}{420}(840\rho l + 2b\rho_c c^3 + 18b\rho_c d c^2 \\
 & \quad + 51b\rho_c d^2 c)\ddot{w}_{a,xx} - 2EIw_{a,xxxx} - b(2\rho d + \rho_c c)\ddot{w}_a \\
 & \quad - \frac{1}{420}b\rho_c c^2(9d/G_c + 2c/G_c + 35c/E_c)\ddot{\tau}_x + b(c+d)\tau_x = -(p_t \\
 & \quad + p_b)
 \end{aligned} \tag{6}$$

$$\begin{aligned}
 & \frac{1}{70}b\rho_c c^2(3/G_c + 14/E_c)\ddot{u}_a + 2bu_a + \frac{1}{420}b\rho_c c^2(9d/G_c + 2c/G_c \\
 & \quad - 42d/E_c - 7c/E_c)\ddot{w}_{a,x} - b(c+d)w_{a,x} + \frac{1}{210}b\rho_c c^3(21/E_c G_c \\
 & \quad - 1/G_c^2)\ddot{\tau} - (bc^3/12E_c)\tau_{,xx} + bc/G_c \tau = 0
 \end{aligned} \tag{7}$$

where u_s , w_s and u_a , w_a are the symmetric and antisymmetric displacement components of the face sheets, τ is the shear stress in the core, EA and EI are the axial and flexural rigidities of the face sheets, respectively, A and I are the cross-sectional area and second moment of inertia of the face sheet, respectively, $(\cdot)_{,x}$ and $(\ddot{\cdot})$ denote the derivative with respect to the spatial coordinate x and the second derivative with respect to time, respectively, b is the width of the beam, c is the height of the



core, d is the thickness of the face sheet, E_c and G_c are the elastic and shear moduli of the core, respectively, ρ is the material density of the face sheet, ρ_c is the material density of the core, $p_i(x, t)$ is the sound pressure acting on the face sheet, and t is the time coordinate [10].

The symmetric and antisymmetric impedances of the sandwich panel can be calculated from Eqs. 3, 4, 5, 6, 7 after using the harmonic wave forms of the pressures and the displacements in the equations

$$\bar{Z} = -\frac{P_t + P_b}{i\omega\bar{W}} \quad (8)$$

$$\tilde{Z} = -\frac{P_t - P_b}{i\omega\tilde{W}} \quad (9)$$

where \tilde{Z} is the impedance of the antisymmetric motion of the sandwich panel, \bar{Z} is the impedance of the symmetric motion of the sandwich panel, P_t and P_b are the amplitudes of the sound pressures on the upper and lower surface of the sandwich panel, and \bar{W} and \tilde{W} represent the amplitudes of the transverse displacements of the symmetric (w_s) and antisymmetric (w_a) motions, respectively. More information about the consistent HSAPT approach and the above equations can be found in Refs. 10, 20.

The antisymmetric and symmetric impedances determined in Eqs. 8, 9 will be used to calculate the wave number, and finally, the sound transmission loss of the sandwich panel, as described in Sec. 3.



3. SEA Equations

The sound transmission between two rooms coupled by a common panel is treated as a three-way coupled system, which is shown schematically in Fig. 2. Subsystem 1 is the ensemble of modes of the diffuse, reverberant sound field in the source room. Subsystem 2 is an appropriately chosen group of vibration modes of the panel. Subsystem 3 is the ensemble of modes of the diffuse reverberant sound field in the receiving room. Sound is generated by a loudspeaker in the source room, which is transmitted through the panel to the receiving room.

For a homogeneous single-layer panel, both W_{12} and W_{23} are related to the bending velocity of the panel. Based on the discussion in Sec. 2, the vibration of the sandwich panel consists not only of the bending mode, but also the dilatational mode.

Therefore, for a sandwich panel, subsystem 2 in Fig. 2 should be further divided into two subsystems that represent the antisymmetric (\sim) and symmetric ($-$) motions, as illustrated in Fig. 3, where subsystems $\tilde{2}$ and $\bar{2}$ represent the appropriately chosen groups of antisymmetric and symmetric vibration modes of the sandwich panel. The notations (\sim) and ($-$) represent the powers related to subsystems $\tilde{2}$ and $\bar{2}$, respectively.



Loudspeaker input power

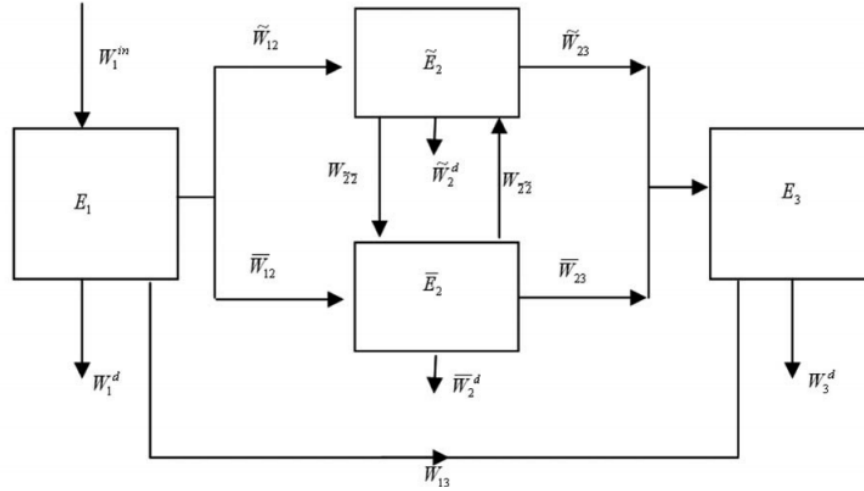


Figure 3: Block diagram illustrating the power flow in four-way coupled systems

The power balance of the subsystems in Fig. 3 is given by the following three algebraic equations:

$$W_1^{\text{inc}} = \tilde{W}_{12} + \bar{W}_{12} + W_{1d} \quad (10)$$

$$\tilde{W}_{12} = \tilde{W}_{2d} + \tilde{W}_{23} + W_{22} \quad (11)$$

$$\bar{W}_{12} = \bar{W}_{2d} + \bar{W}_{23} + W_{2\bar{2}} \quad (12)$$

By combining Eqs. 11, 12, the total power transmitted from the source room through the sandwich panel into the receiving room is

$$\tilde{W}_{12} + \bar{W}_{12} = \tilde{W}_{2d} + \bar{W}_{2d} + \tilde{W}_{23} + \bar{W}_{23} \quad (13)$$

Note that W_{13} in Fig. 3 represents the transmission of sound by the mass law. Because the SEA method accounts for the energy flow through the resonant modes, W_{13} is neglected in the equations



above. However, W_{13} will be included when calculating the sound transmission coefficient, as described next.

The total energies in subsystems 1 and 2 are given by

$$E_1 = \frac{\langle p_1^2 \rangle}{\rho c^2} V \quad (14)$$

$$\tilde{E}_2 = \rho_s S \langle \tilde{v}^2 \rangle \quad (15)$$

$$\bar{E}_2 = \rho_s S \langle \bar{v}^2 \rangle \quad (16)$$

where $\langle p_1^2 \rangle$ represents the mean-square sound pressure in the source room, V is the volume of the source room, $\langle \tilde{v}^2 \rangle$ and $\langle \bar{v}^2 \rangle$ denote the mean-square panel vibration velocities of the antisymmetric and symmetric motions, respectively, S is the panel surface area, and ρ_s is the mass per unit area of the sandwich panel.

The reverberant sound power incident on the sandwich panel is

$$W_1^{\text{inc}} = \frac{\langle p_1^2 \rangle}{4\rho c} S \quad (17)$$

The power dissipated in a subsystem is related to the energy stored by that subsystem E_i through the dissipative loss factor η_i in the relation

$$W_i^d = E_i \omega \eta_i \quad (18)$$

The net power flow from system i to system j is



$$W_{ij} = \omega \eta_{ij} n_i \left(E_i^m - E_j^m \right) \quad (19)$$

where η_{ij} is the coupling loss factor from subsystem i to subsystem j , and n_i is the modal density of subsystem i . They obey the reciprocity rule

$$\frac{\eta_{ij}}{\eta_{ji}} = \frac{n_j}{n_i} \quad (20)$$

Therefore, for the sandwich panel under study

$$\bar{W}_{12} = \omega \eta_{12} \bar{n}_1 \left(\frac{E_1}{n_1} - \frac{\bar{E}_2}{\bar{n}_2} \right) = \omega \bar{\eta}_{21} \bar{n}_2 \left(\frac{E_1}{n_1} - \frac{\bar{E}_2}{\bar{n}_2} \right) \quad (21)$$

$$\bar{W}_{12} = \omega \eta_{12} \bar{n}_1 \left(\frac{E_1}{n_1} - \frac{\bar{E}_2}{\bar{n}_2} \right) = \omega \bar{\eta}_{21} \bar{n}_2 \left(\frac{E_1}{n_1} - \frac{\bar{E}_2}{\bar{n}_2} \right) \quad (22)$$

The power that the plate radiates into the receiving room, having been excited into vibration by the sound power from the source room, is given by W_{23} . Thus

$$\bar{W}_{23} = \langle \bar{v}^2 \rangle \rho c \bar{\sigma}_{\text{rad}} S \equiv \bar{E}_2 \omega \bar{\eta}_{23} \quad (23)$$

$$\bar{W}_{23} = \langle \bar{v}^2 \rangle \rho c \bar{\sigma}_{\text{rad}} S \equiv \bar{E}_2 \omega \bar{\eta}_{23} \quad (24)$$

Substituting Eqs. (14)-(16), (18), and (21)-(24) into Eq. (13) yields the following equation:

$$\begin{aligned} & \omega (\bar{\eta}_{21} \bar{n}_2 + \bar{\eta}_{21} \bar{n}_2) \frac{E_1}{n_1} S_2 [(\rho_s \omega \bar{\eta}_2 + \rho_s \omega \bar{\eta}_{21} + \rho c \bar{\sigma}_{\text{rad}}) \langle \bar{v}^2 \rangle + (\rho_s \omega \bar{\eta}_2 \\ & + \rho_s \omega \bar{\eta}_{21} + \rho c \bar{\sigma}_{\text{rad}}) \langle \bar{v}^2 \rangle] \end{aligned} \quad (25)$$

Please cite this article as: Wang T, Li S, Rajaram S, Nutt SR. **Predicting the Sound Transmission Loss of Sandwich Panels by Statistical Energy Analysis Approach.** *ASME. J. Vib. Acoust.* 2010;132(1):011004-011004-7. doi:10.1115/1.4000459.



The coupling loss factors $\tilde{\eta}_{23}$ and $\bar{\eta}_{23}$ can be calculated from Eqs. 23, 24. The sandwich panel is coupled to both rooms by sound radiation. Therefore

$$\tilde{\eta}_{21} = \tilde{\eta}_{23} = \frac{\rho c \bar{\sigma}_{\text{rad}}}{\rho_s \omega} \quad (26)$$

$$\bar{\eta}_{21} = \bar{\eta}_{23} = \frac{\rho c \bar{\sigma}_{\text{rad}}}{\rho_s \omega} \quad (27)$$

The modal densities are calculated from [13]

$$\bar{n}_2 = \frac{\omega S}{2\pi \bar{c}_\phi \bar{c}_g} \quad (28)$$

$$\tilde{n}_2 = \frac{\omega S}{2\pi \tilde{c}_\phi \tilde{c}_g} \quad (29)$$

where $\tilde{c}_\phi = \omega/\tilde{k}$ and $\tilde{c}_g = d\omega/d\tilde{k}$ are the phase and group speeds for the bending wave traveling in the sandwich panel, and $\bar{c}_\phi = \omega/\bar{k}$ and $\bar{c}_g = d\omega/d\bar{k}$ are the phase and group speeds for the dilatational wave in the sandwich panel.

The relationship between the bending \tilde{v} and the dilatational \bar{v} velocities are derived from Eqs. (20)–(21) and (30)–(31) in Ref. 10

$$\bar{v} = \frac{p_t + p_b}{\bar{Z}} \quad (30)$$

$$\tilde{v} = \frac{p_t - p_b}{\tilde{Z}} \quad (31)$$

$$p_t = 2p_i - Z_{\text{air}}(\tilde{v} + \bar{v}) \quad (32)$$

$$p_b = Z_{\text{air}}(\tilde{v} - \bar{v}) \quad (33)$$

Please cite this article as: Wang T, Li S, Rajaram S, Nutt SR. **Predicting the Sound Transmission Loss of Sandwich Panels by Statistical Energy Analysis Approach.** *ASME. J. Vib. Acoust.* 2010;132(1):011004-011004-7. doi:10.1115/1.4000459.



where Z_{air} is the impedance of air, and p_i represents the incident sound pressure on the upper face sheet.

From Eqs. (30)–(33)

$$p_t + p_b = 2p_i - 2Z_{air}\bar{v} = \bar{Z}\bar{v} \quad (34)$$

$$p_t - p_b = 2p_i - 2Z_{air}\bar{v} = \bar{Z}\bar{v} \quad (35)$$

Therefore

$$2p_i = (\bar{Z} + 2Z_{air})\bar{v} = (\bar{Z} + 2Z_{air})\bar{v} \quad (36)$$

Which yields

$$(2Z_{air} + \bar{Z})\bar{v} = (2Z_{air} + \bar{Z})\bar{v} \quad (37)$$

Substituting Eqs. (14), (26)–(29), and (37) into Eq. (25), the relationship between $\langle \tilde{v}_2 \rangle$ and $\langle p_1^2 \rangle$

$$\frac{\langle \tilde{v}_2^2 \rangle}{\langle p_1^2 \rangle} = \frac{\pi c^2 \left(\frac{\bar{\sigma}_{rad}}{\bar{c}_\phi \bar{c}_g} + \frac{\bar{\sigma}_{rad}}{\bar{c}_\phi \bar{c}_g} \right)}{\rho_s \omega \left[(\rho_s \omega \bar{\eta}_2 + 2\rho c \bar{\sigma}_{rad}) + \frac{\bar{Z} + 2Z_{air}}{\bar{Z} + 2Z_{air}} (\rho_s \omega \bar{\eta}_2 + 2\rho c \bar{\sigma}_{rad}) \right]} \quad (38)$$

The transmitted energy W_{13} given by the mass law, depends only on the areal mass density of the sandwich panel, and is calculated by the formula below [15]

$$W_{13} = \langle p_1^2 \rangle \frac{\pi \rho c S}{\rho_s^2 \omega^2} \quad (39)$$

The sound transmission coefficient is defined as the ratio between the transmitted and incident sound powers, which can be represented as

$$\tau = \frac{\bar{W}_{23} + \bar{W}_{23} + W_{13}}{W_{inc}} \quad (40)$$

Please cite this article as: Wang T, Li S, Rajaram S, Nutt SR. **Predicting the Sound Transmission Loss of Sandwich Panels by Statistical Energy Analysis Approach.** *ASME. J. Vib. Acoust.* 2010;132(1):011004-011004-7. doi:10.1115/1.4000459.



From Eqs. (17), (23), (30), and (39)

$$\tau = \frac{\rho c [\langle \bar{v}^2 \rangle \bar{\sigma}_{\text{rad}} + \langle \bar{v}^2 \rangle \bar{\sigma}_{\text{rad}}] S + \langle p_1^2 \rangle \frac{\pi \rho c S}{\rho_s^2 \omega^2}}{\frac{\langle p_1^2 \rangle}{4 \rho c} S + \frac{\bar{Z} + 2Z_{\text{air}}}{\bar{Z} + 2Z_{\text{air}}} \bar{\sigma}_{\text{rad}}} \left(\frac{\langle \bar{v}^2 \rangle}{\langle p_1^2 \rangle} + \frac{4 \pi \rho^2 c^2}{\rho_s^2 \omega^2} \right) \quad (41)$$

Substituting Eq. 38 into Eq. 41, the sound transmission coefficient is calculated. The transmission coefficient τ is a function of the incident angle θ . To account for the incident sound waves from all directions of a diffuse sound field, the sound transmission coefficient is averaged with respect to the azimuthal angles

$$\hat{\tau} = \frac{\int_0^{\theta_0} \tau(\theta) \sin \theta \cos \theta d\theta}{\int_0^{\theta_0} \sin \theta \cos \theta d\theta} \quad (42)$$

where $\hat{\tau}$ is the averaged field-incidence transmission coefficient and $\theta_0 = 78$ deg is the empirically determined upper bound of the incident angle.

Finally, the sound transmission loss is calculated using

$$\text{STL} = 10 \log \left(\frac{1}{\hat{\tau}} \right) \quad (43)$$

4. Numerical Examples

Table 1: Mechanical and geometrical properties of the sandwich panel [5]

Property	Panel A
Young's modulus of the face sheet (MPa)	7000
Density of the face sheet (kg/m ³)	629.9
Thickness of the face sheet (mm)	6.35

Please cite this article as: Wang T, Li S, Rajaram S, Nutt SR. **Predicting the Sound Transmission Loss of Sandwich Panels by Statistical Energy Analysis Approach.** ASME. *J. Vib. Acoust.* 2010;132(1):011004-011004-7. doi:10.1115/1.4000459.



Young's modulus of the core (MPa)	8.3
Shear modulus of the core (MPa)	3.1
Density of the core (kg/m ³)	16
Thickness of the core (mm)	38.1

A sandwich panel (panel A) was used as a numerical example to calculate the transmission loss with the present SEA approach, the properties of which are listed in Table 1. The sound transmission loss was predicted and compared with experimental data and with predictions generated using other SEA approaches. The key parameter for the SEA approach is the wave number of the traveling wave in the structure. From knowledge of this parameter, the wave speed, radiation efficiency, and modal density can be determined and used to calculate the sound transmission loss.

4.1 Impedances

The consistent HSAPT approach was utilized in the calculation to consider both the antisymmetric and symmetric motions of the sandwich panel. First, the antisymmetric \tilde{Z} and symmetric \bar{Z} impedances of the sandwich panel were calculated from Eqs. 8, 9. The expressions for the impedances were neglected here because of the complexity of the equations. The impedances, both symmetric and antisymmetric, are purely imaginary, as long as no damping is included. The amplitudes of the symmetric and antisymmetric impedances of panel A are displayed in Fig. 4 for normal incidence.

The antisymmetric impedance is smaller than the symmetric impedance at low frequency, so the panel behaves mostly in bending motion below 1000 Hz. At frequencies above 1000 Hz, the dilatational mode becomes more prominent, especially when the symmetric impedance is less than the antisymmetric impedance at ~1700–2000 Hz. At still higher frequencies, the two impedances



tend to coincide, indicating that the dilatational modes are comparable in amplitude to the bending modes of the sandwich panel motions. The cause of this phenomenon will be discussed next.

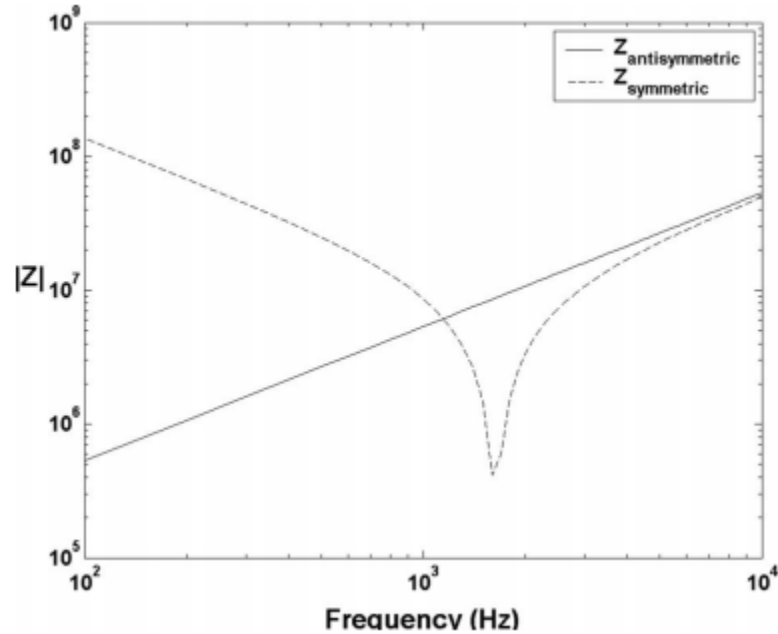


Figure 1: Impedances for panel A: $Z_{antisymmetric} = \tilde{Z}$ and $Z_{symmetric} = \bar{Z}$

At a frequency of ~ 1500 Hz, the two impedances are equal. Referring to Fig. 1 and Eq. 2, this means $w_b = \tilde{w} - \bar{w} \approx 0$. The lower face sheet does not move regardless of the external excitation on the upper face sheet, which indicates little sound transmission through the sandwich panel. Correspondingly, there is a peak in the sound transmission loss curve around that frequency, as will be shown in Fig. 8.

4.2 Wave Number and Wave Speed

For a particular frequency ω , equating the impedances to zero leads to two equations in terms of the antisymmetric and symmetric wave numbers (\tilde{k} and \bar{k})

Please cite this article as: Wang T, Li S, Rajaram S, Nutt SR. **Predicting the Sound Transmission Loss of Sandwich Panels by Statistical Energy Analysis Approach.** *ASME. J. Vib. Acoust.* 2010;132(1):011004-011004-7. doi:10.1115/1.4000459.



$$\tilde{Z}(\tilde{k}) = 0 \tag{44}$$

$$\bar{Z}(\bar{k}) = 0 \tag{45}$$

Real positive roots of Eqs. 44, 45 yield the antisymmetric and symmetric wave numbers for the particular frequency ω . A dispersive wave number versus frequency curve was obtained by repeating this calculation for every third octave band frequency. The phase wave speed can be calculated from the wave number

$$c_\phi = \omega/k \tag{46}$$

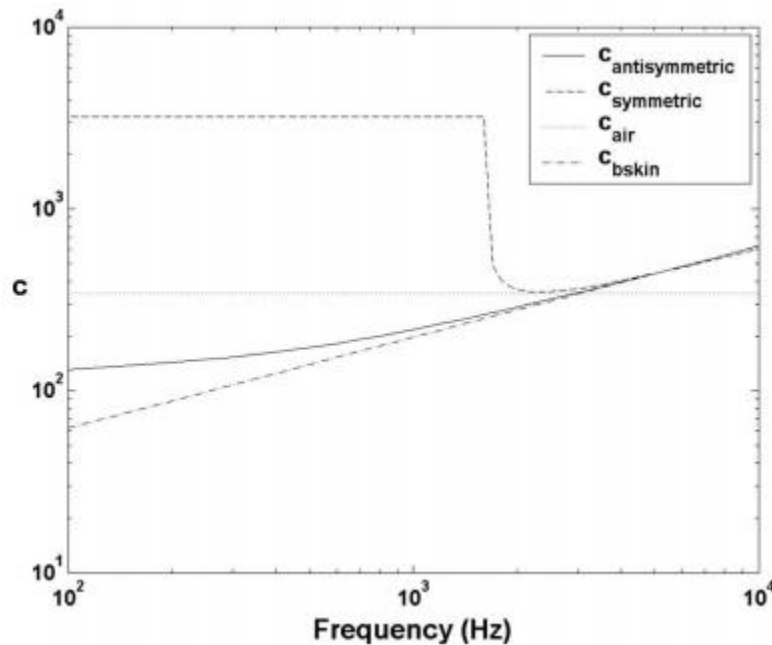


Figure 5: Wave speeds of panel A, where $c_{antisymmetric}$ represents the antisymmetric wave phase speed \bar{c}_ϕ , $c_{symmetric}$ denotes the symmetric phase speed \tilde{c}_ϕ , c_{air} is the wave speed of sound in the air, and $c_{b\ skin}$ is the bending wave speed for the bending of skin loaded with half of the core mass



A comparison of the wave speeds of panel A with the speed of sound in the air is given in Fig. 5. The antisymmetric wave speed \tilde{c}_ϕ increases with frequency and coincides with the speed of sound in the air at ~ 3000 Hz. The symmetric wave speed \bar{c}_ϕ is constant at low frequency and much greater than the speed of sound in air. The constant wave speed at low frequency derives from the longitudinal wave propagating in the thickness direction of the sandwich panel, because there is no dilatational motion in the sandwich panel yet. Because the symmetric wave speed is always greater than the speed of sound in the air, the symmetric coincidence occurs at ~ 2000 Hz when the first dilatational mode occurs. The dilatation frequency f_d is defined as [4]

$$f_d = \frac{1}{2\pi} \left[\left(\frac{2K}{c} \right) / \left(\rho d + \frac{\rho_c c}{6} \right) \right]^{1/2} \quad (47)$$

where $K = (E_c(1-\nu_c)/(1+\nu_c)(1-2\nu_c))$ is the longitudinal modulus of the core. Using the material properties defined in Table 1, $f_d = 2030$ Hz.

At high frequency, both the antisymmetric and symmetric wave speeds vary asymptotically with $c_{b \text{ skin}}$, the bending wave speed of a skin loaded with half of the core mass [17]

$$c_{b \text{ skin}} = \sqrt{\omega} \left[\frac{B_1}{(\rho_s/2)} \right]^{1/4} \quad (48)$$

Where $B_1 = (E/12(1-\nu^2))d^3$ is the bending stiffness of the face sheet. This is consistent with previous results obtained in Refs. [2, 4, 5, 17].

At high frequency, there are multiple resonant modes for both antisymmetric and symmetric motions of the sandwich panel. The sandwich panel can be viewed as a double-wall structure, with each “wall” comprised of one face sheet and half of the core. Both antisymmetric and symmetric



waves propagate in the sandwich panel, and both are related to the bending speed of each wall. As the two walls bend in phase, the sandwich panel appears to be in antisymmetric motion, and when they bend out of phase, the dilatational motion is observed. Therefore, the difference in wave speed is expected to be negligible, while different vibration modes are observed as the two walls vibrate in phase or out of phase with each other. This is the reason for the equivalence of the antisymmetric and symmetric impedances at high frequencies, as described above.

The group wave speeds c_g were also determined from the wave numbers by $c_g = d\omega/dk = (1/dk/d\omega)$. The group wave speeds of panel A are plotted in Fig. 6. These are not equal to the phase wave speeds of panel A because the waves are dispersive. The modal densities of the sandwich panel can be calculated from the phase and group wave speeds by Eqs. 28, 29.

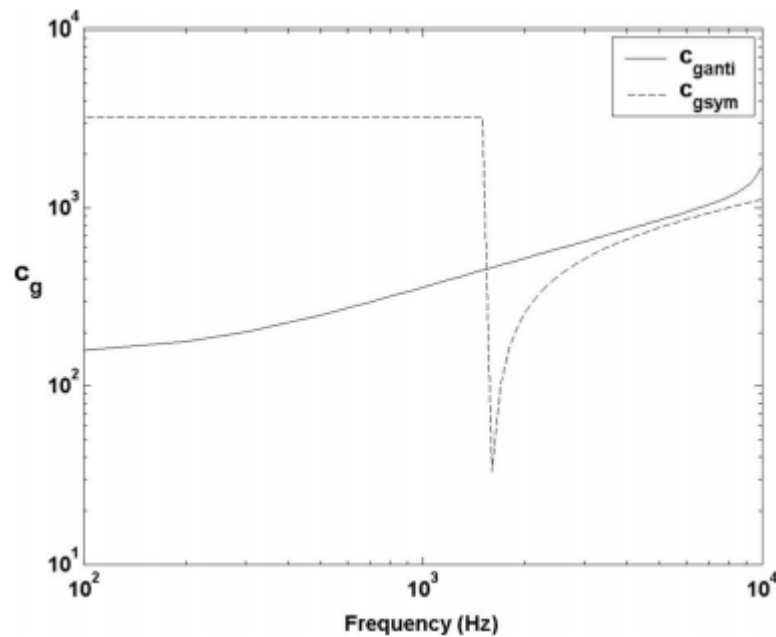


Figure 6: Group wave speeds of panel B, where $c_{g\ anti}$ represents the group wave speed for the antisymmetric motion \tilde{c}_g and $\tilde{c}_{g\ sym}$ denotes the symmetric group wave speed \tilde{c}_g



4.3 Radiation Efficiency

The radiation efficiency is defined as the ratio of the sound power radiated by the structure to the sound power radiated by a piston of equal area of radiation. The radiation efficiency depends on the wave number. Lyon and DeJong's formula [13] was used to calculate the radiation efficiency of the bending motion of the sandwich panel below the antisymmetric coincident frequency

$$\bar{\sigma}_{\text{rad}} = \frac{2 L_s}{\pi S} \frac{k_0^2}{\bar{k}^3 \left(1 + \frac{\pi k_0^2}{2 \bar{k}^2} \right)} + \frac{1}{\sqrt{\left(\frac{\bar{k}^2}{k_0^2} - 1 \right)^2 \left(\frac{\pi \bar{k}^4}{k_0^4} + 1 \right)^2 + \frac{2 \pi}{\bar{k} \sqrt{S}}}} \quad (49)$$

where L_s is the perimeter of the sandwich panel, and k_0 is the wave number of sound in the air.

Above the antisymmetric critical frequency, the antisymmetric radiation efficiency goes asymptotically to value 1

$$\bar{\sigma}_{\text{rad}} = \frac{1}{(1 - f_c/f)^{1/2}} \quad (50)$$

As discussed above, there is no dilatational motion below f_d , which is the first resonant frequency for the symmetric motion. The radiation efficiency of the symmetric motion is therefore approximated as

$$\bar{\sigma}_{\text{rad}} = 0 \quad \text{if } f < f_d \quad (51)$$

$$\bar{\sigma}_{\text{rad}} = 1 \quad \text{if } f \geq f_d \quad (52)$$



The radiation efficiencies of panel A are shown in Fig. 7. The antisymmetric radiation efficiency increases gradually with frequency. As the frequency increases, more and more resonant modes occur in the structure and the structure becomes a better noise radiator. At the coincident frequency, the speed of sound in air matches the speed of sound waves in the structure, which enables the structure to be an efficient sound radiator. Thus, at this frequency, the sound radiation efficiency reaches a maximum. The symmetric radiation efficiency is defined by Eqs. (51) and (52).

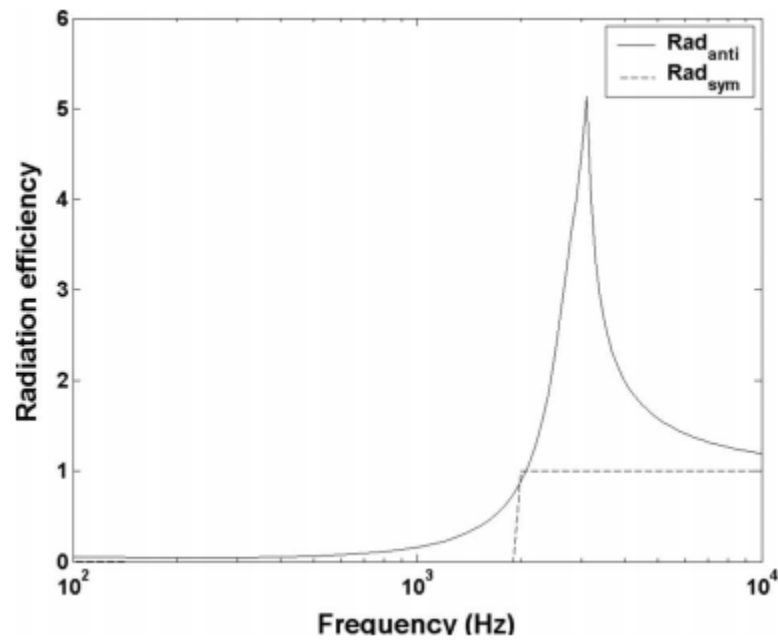


Figure 7: Radiation efficiencies of panel A, where Rad_{anti} represents the antisymmetric radiation efficiency $\tilde{\sigma}_{rad}$ and Rad_{sym} denotes the radiation efficiency for the symmetric motion $\bar{\sigma}_{rad}$

4.4 Sound Transmission Loss

Finally, the sound transmission loss of panel A was calculated from Eq. (43) and these results are compared with the experimental data in Fig. 8. Also included is the TL predictions obtained by a

Please cite this article as: Wang T, Li S, Rajaram S, Nutt SR. **Predicting the Sound Transmission Loss of Sandwich Panels by Statistical Energy Analysis Approach.** ASME. *J. Vib. Acoust.* 2010;132(1):011004-011004-7. doi:10.1115/1.4000459.



simpler SEA approach described in Ref. [17]. The present prediction matches the measured experimental data well. Both the symmetric coincident frequency (2000 Hz) and the antisymmetric coincident frequency (3000 Hz) were predicted by the present approach, while only the antisymmetric coincident frequency was predicted by the previous SEA approach in Ref. [17]. The shortcoming of the simpler SEA approach arises because the sandwich panel was assumed to be single-layer and homogeneous, while the present SEA approach considers both the antisymmetric and symmetric motions of the sandwich panel.

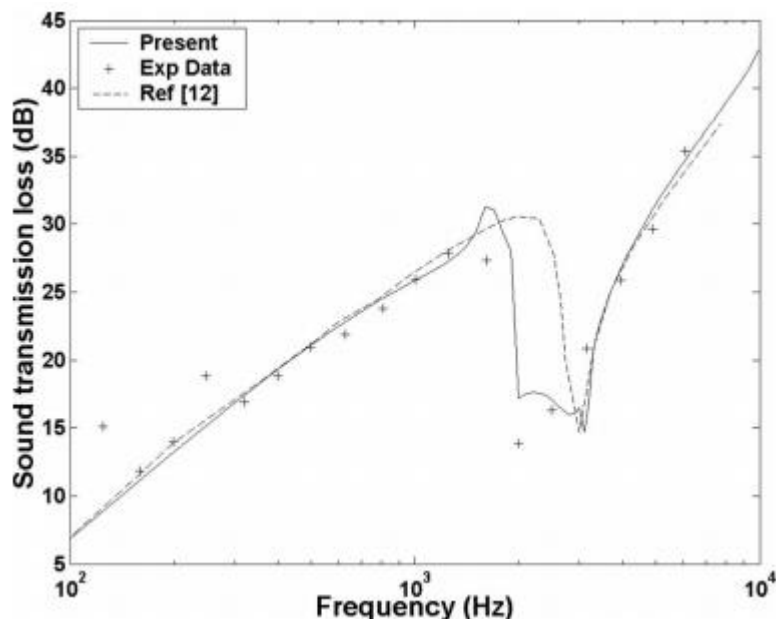


Figure 8: Sound transmission loss of panel A, where – represents the prediction of the present SEA approach, + represents the experimental data [6], -- represents the prediction of the SEA approach in Ref. [12]

5. Conclusions

The sound transmission loss of symmetric sandwich panels was predicted using a SEA approach.

Unlike conventional SEA, the current approach considered both antisymmetric and symmetric

Please cite this article as: Wang T, Li S, Rajaram S, Nutt SR. **Predicting the Sound Transmission Loss of Sandwich Panels by Statistical Energy Analysis Approach**. *ASME. J. Vib. Acoust.* 2010;132(1):011004-011004-7. doi:10.1115/1.4000459.



motions of the panel, and these motions were treated independently. The wave number, wave speed, and radiation efficiency for both antisymmetric and symmetric motions were predicted. When compared with experimentally measured TL, the predicted sound transmission loss results yield superior agreement compared with conventional SEA.

The present SEA approach overcomes a shortcoming of conventional SEA approaches, by accounting for symmetric motions of the sandwich panel. In addition, the present approach can be used to predict additional acoustic properties, such as the modal density, wave speed, and radiation efficiency. These capabilities can be applied to studies of sandwich panel vibration and radiation. Future work will be devoted to optimizing the design of sandwich panels for acoustic and mechanical properties.

Acknowledgements: The authors are grateful to the Merwyn C. Gill Foundation for support of this research.

References:

1. Dym, C. L., and Lang, M. A., 1983, "Transmission Loss of Damped Asymmetric Sandwich Panels With Orthotropic Cores," *J. Sound Vib.*, 88 (3), pp. 299–319.
2. Kurtze, G., and Watters, B. G., 1959, "New Wall Design for High Transmission Loss or High Damping," *J. Acoust. Soc. Am.*, 31 , pp. 739–748.
3. Ford, R. D., Lord, P., and Walker, A. W., 1967, "Sound Transmission Through Sandwich Constructions," *J. Sound Vib.*, 5 (1), pp. 9–21.
4. Dym, C. L., and Lang, M. A., 1974, "Transmission of Sound Through Sandwich Panels," *J. Acoust. Soc. Am.*, 56 (5), pp. 1523–1532.
5. Moore, J. A., 1975, "Sound Transmission Loss Characteristics of Three Layer Composite Wall Constructions," Ph.D. thesis, Massachusetts Institute of Technology, Cambridge, MA.
6. Narayanan, S., and Shanbhag, R. L., 1982, "Sound Transmission Through a Damped Sandwich Panel," *J. Sound Vib.*, 80 , pp. 315–327.
7. Nilsson, A. C., 1990, "Wave Propagation in and Sound Transmission Through Sandwich Plates," *J. Sound Vib.*, 138 (1), pp. 73–94.
8. Thamburaj, P., and Sun, J. Q., 1999, "Effect of Material Anisotropy on the Sound and Vibration Transmission Loss of Sandwich Aircraft Structures," *J. Sandwich. Struct. Mater.*, 1 , pp. 76–92.
9. Thamburaj, P., and Sun, J. Q., 2001, "Effect of Material and Geometry on the Sound and Vibration Transmission Across a Sandwich Beam," *Trans. ASME, J. Vib. Acoust.*, 123 , pp. 205–212.

Please cite this article as: Wang T, Li S, Rajaram S, Nutt SR. **Predicting the Sound Transmission Loss of Sandwich Panels by Statistical Energy Analysis Approach.** *ASME. J. Vib. Acoust.* 2010;132(1):011004-011004-7. doi:10.1115/1.4000459.



10. Wang, T., Sokolinsky, V., Rajaram, S., and Nutt, S. R., 2005, "Assessment of Sandwich Models for the Prediction of Sound Transmission Loss in Unidirectional Sandwich Panels," *Appl. Acoust.*, 66 (3), pp. 245–262.
11. Papadopoulos, C. I., 2003, "Development of an Optimized Standard-Compliant Procedure to Calculate Sound Transmission Loss: Numerical Measurements," *Appl. Acoust.*, 64 , pp. 1069–1085.
12. Li, S., Wang, T., and Nutt, S. R., 2005, "Transmission Loss Assessments of Sandwich Structures by Using a Combination of Finite Element and Boundary Element Methods," *NOISE-CON 2005* , Minneapolis, MN, Oct. 17–19.
13. Lyon, R. H., and DeJong, R. G., 1998, "*Theory and Application of Statistical Energy Analysis*", 2nd ed., R. H. Lyon Corp., Cambridge, MA.
14. Renji, K., Nair, P. S., and Narayanan, S., 1996, "Modal Density of Composite Honeycomb Sandwich Panels," *J. Sound Vib.*, 195 (5), pp. 687–699.
15. Beranek, L. L., and Ver, I. L., 1992, "*Noise and Vibration Control Engineering—Principles and Applications*", Wiley, New York.
16. Crocker, M. J., and Price, A. J., 1969, "Sound Transmission Using Statistical Energy Analysis," *J. Sound Vib.*, 9 (3), pp. 469–486.
17. Patil, A. R., 2000, "Sound Radiation and Transmission Characteristics of finite Composite Panels," Ph.D. thesis, Auburn University, Auburn, AL.
18. Ghinet, S., Atalla, N., and Osman, H., 2005, "The Transmission Loss Through Curved Sandwich Composite Structures," *J. Acoust. Soc. Am.*, 118 , pp. 774–790.
19. Ghinet, S., Atalla, N., and Osman, H., 2006, "Diffuse Field Transmission Into Infinite Sandwich Composite and Laminate Composite Cylinders," *J. Sound Vib.*, 289 , pp. 745–778.
20. Sokolinsky, V. S., and Nutt, S. R., 2004, "Consistent Higher-Order Dynamical Equations for Soft-Core Sandwich Beams," *AIAA J.*, 42 (2), pp. 374–382.

Please cite this article as: Wang T, Li S, Rajaram S, Nutt SR. **Predicting the Sound Transmission Loss of Sandwich Panels by Statistical Energy Analysis Approach.** *ASME. J. Vib. Acoust.* 2010;132(1):011004-011004-7. doi:10.1115/1.4000459.